
# Non-stationary Holography on Arbitrary Source Shapes

Jesper GOMES[1]; Yutaka ISHII[2]; Bernard Ginn[3]

[1,3] Brüel & Kjaer SVM A/S, Denmark.

[2] Brüel & Kjaer Japan.

## ABSTRACT

Laser scanning and accelerometer measurements are often used for analysing vibrations of for instance motors under operation. However, the methods have certain disadvantages: Laser techniques typically scan one point at a time, which limits the methods to be applied only for stationary conditions. Accelerometers can be used for non-stationary conditions, but their physical mounting will to some extend influence the vibration of the source surface and due to cabling they are not practical for rotating objects. Near-field Acoustical Holography (NAH) is a non-contact experimental technique for mapping sound and vibration, and since the sound field is measured at multiple points around the source simultaneously, it can also be applied for non-stationary conditions. In particular, the Equivalent Source Method (ESM) is an attractive holography method, because it does not require neither the source nor the array geometry to be given in separable coordinates (planar, spherical, cylindrical etc.). This paper describes a non-stationary ESM approach for reconstruction of quantities like surface velocity and displacement. A set of measurements has been made with a 60 channel microphone array on a small electrical motor. Vibrations were also measured with a laser vibrometer in order to validate the accuracy of the array calculations.

Keywords: Noise Source Identification, Microphone arrays, Array signal processing.
I-INCE Classification of Subjects Numbers: 72, 75.7, 74.7.

## 1. INTRODUCTION

Over the last three decades, microphone array techniques have become very popular for identifying noise sources. These techniques no longer just serve academic purposes, but are also widely used in industries like the automotive, aerospace or consumer product industries. It is an efficient way of getting a quick answer about where sound is radiated from and because the sound is visualized as an acoustical image, it is a powerful way of sharing information between people.

Generally, array techniques can be divided into two groups: holography techniques and beamforming techniques. Holography is for low-to-mid frequencies, whereas beamforming is for mid-to-high frequencies. The upper frequency limit of holography is limited by the microphone spacing: the spacing must be less than half of a wavelength. Beamforming have the ability to go up to frequency ranges where there are two to three wavelengths between neighboring microphones. The disadvantage of beamforming is that the optimal spatial resolution of the reconstructed sound map is approximately equal to one wavelength even when measuring close to the source. The resolution of holography is only limited by – and equal to - the microphone spacing as long as the distance to the source is less than or equal to the spacing. This means that it is possible to get high spatial resolution results at low frequencies. Also, holography can reconstruct quantities like the particle velocity and/or displacement which means that the technique can also be applied for analyzing vibrations on the source. It is therefore an alternative to laser scan or accelerometer measurements.

Near-field Acoustical Holography (NAH) was first introduced in the literature in the early 1980s (1). This traditional approach used Fast Fourier Transform (FFT) to transform the sound field from the spatial domain to the wavenumber domain. In the wave number domain, the sound field can be

[1] Jesper.Gomes@bksv.com

projected to another plane parallel to the measurement plane, and in this new plane, the sound field is transformed back to the spatial domain by applying an inverse FFT. These computations are quite cheap in terms of CPU load, which means that the technique is very suitable for arrays with a lot of measurement points, e.g., when scanning an array over a large area with a robot resulting in thousands of measurement points. The drawback of the method is that it is limited to measurement and calculation surfaces of separable coordinates, i.e., planar, cylindrical, spherical etc.

In the 1990s a different type of holography technique was introduced namely the Inverse Boundary Element Method (IBEM) (2, 3). The idea is to discretize the source surface as boundary elements and set up a system of equations that relates the sound pressure at a set of field points to for instance the particle velocity on the nodes of the boundary elements. In classical Boundary Element Methods (BEMs) the known quantities are the particle velocity at the nodes, which are used to evaluate the field pressure. In IBEM the aim is to solve the inverse problem: it is the field sound pressure values that are used to predict surface velocities on the source surface by solving the inverse problem. This method is more computationally demanding than FFT-based NAH, but has the advantage that it works on arbitrary/non-separable source geometries.

Another type of holography technique called Equivalent Source Method (ESM) was introduced around one decade ago (4, 5). The idea is to represent the sound source as a set of equivalent monopole sources distributed on virtual surface, which is retracted from the actual source surface. The complex amplitudes of these monopoles are estimated by fitting them to the sound field measured by the array. After finding the amplitudes, the sound pressure and/or particle velocity can be evaluated directly on the source surface. As shown in reference (5) the ESM algorithm can in fact be seen as an approximation to IBEM, and it turns out that the method performs very well despite its simplicity

Holography algorithms are typically formulated in the frequency domain, but they can also be applied for analyzing phenomena in the time-domain (6-8). One approach is to apply an FFT on the array signals, solve the holography problem in the frequency domain followed by an inverse FFT to get back into the time domain (7). It is also possible to solve the holography problem directly in the time domain as in Reference (8). Non-stationary holography is more computationally demanding than the stationary one, which is why FFT-based holography is a good choice in terms of performance. However, if the source geometry is irregular ESM is attractive due to its simplicity and applicability on arbitrary sources. This paper describes a system that uses non-stationary ESM, and the method is demonstrated on a small operating electrical motor. Although the motor and the array has a cylindrical shape, which makes it suitable for FFT-based NAH, the source could as well have had a more irregular shape without suffering on accuracy.

## 2. THEORY

This paper describes an implementation of a non-stationary ESM implementation which is called Proximal Holography. The word “Proximal” refers to the fact that the microphones are oriented towards the source following the overall trend of the source shape, but not necessarily being completely conformal to the source surface. This is illustrated in the example sketch in Figure 1.

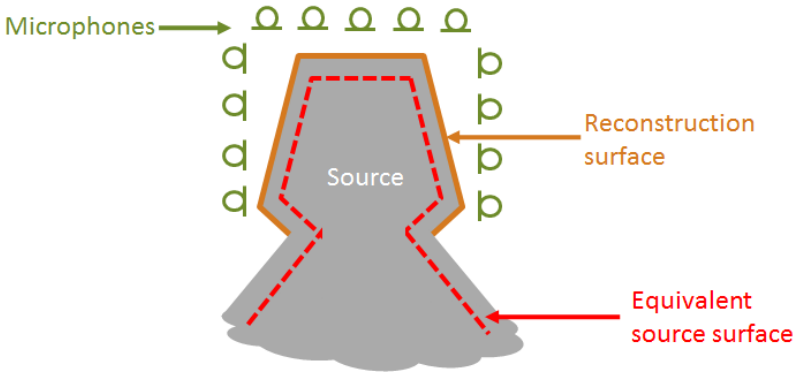


Figure 1 – Illustration of the principle of Proximal Holography based on ESM.

In the ideal world the standoff distance to the array is constant and equal to 0.5-1 times the

microphone spacing, and the microphones cover the entire structure under test. This gives the highest accuracy over the structure. Often in real-life scenarios, though, the ideal setup is not easy to realize. Firstly, only a part of the vibrating source may be of interest and covering all parts of the source would be time consuming and/or expensive in terms of hardware. Secondly, the shape of the source may be very irregular making it complicated to design an array that follows the physical surfaces. To meet these practical issues a "proximal array" can be used as long as the trend of the source shape is followed and the source must be within a reasonable short distance from the array (for instance 2-3 times the microphone spacing). Notice also in Figure 1 that only a part of the source is covered by microphones, whereas the equivalent source surface is larger. The purpose of the equivalent source surface is to be able to represent the sound field in the domain near the array and reconstruction surface. Sources that are not directly below the array may still contribute to the sound field measured by the array, which is why the equivalent sources must go beyond the array to model this part of the field. On the other hand, areas that are much further away are likely not to contribute to the sound measured at the array, and the virtual source surface can therefore be truncated at some distance from the outermost microphones. Typical truncation distances are 3-4 microphone spacings beyond the array edge. The reconstruction surface is generally recommend not to extend beyond the area covered by the array.

### 2.1 Data Workflow

To get a time domain output from the Proximal Holography method, a data workflow similar to that of Reference 7 is used. The processing blocks are illustrated in Figure 2.

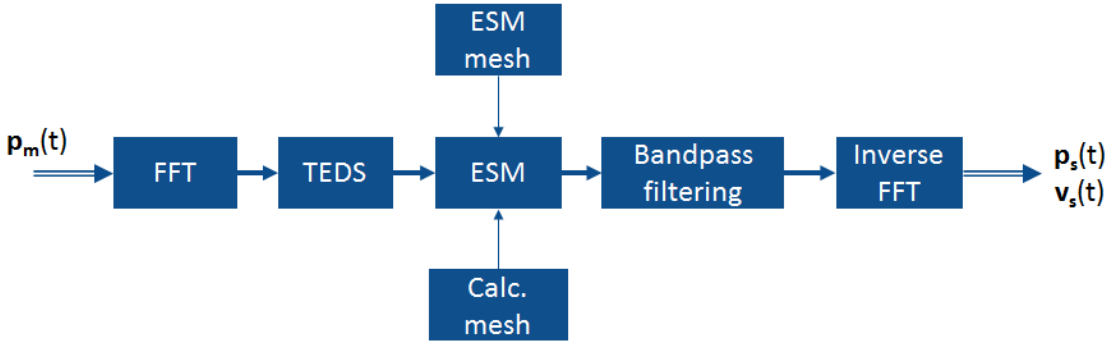


Figure 2 – Dataflow in Transient Proximal Holography. Input is sound pressure recordings from the array microphones and the default outputs are pressure and particle velocity time histories.

The measured time signals from the array are transformed to the frequency domain via the FFT, and then each microphone's unique "Transducer Electronic Data Sheet" (TEDS) information is read from the transducer and the correction data is applied to the measured spectra. The ESM algorithm takes these frequency spectra as input together with a mesh of equivalent sources and the mesh on which the sound field is to be projected, and processes the data frequency line by frequency line. Then each frequency band of interest is filtered independently and the filtered spectra are transformed back to the time domain by use of the inverse FFT. Although not explicitly shown in Figure 2, padding and a Gauss window is applied before the FFT to avoid spectral leakage and an inverse window is applied after the Inverse FTT. The ESM output is pressure and particle velocity, but the displacement on the source is an alternative output which is easily computed by dividing the particle velocity by $j\omega$ (where $\omega$ is the angular frequency) before performing the Inverse FFT. From the complex pressure and velocity, $\mathbf{p}_s(t)$ and $\mathbf{v}_s(t)$, the instantaneous intensity and/or envelope intensity can also be evaluated (7). The calculated quantities can be displayed and animated as a function of time in order to analyze transient phenoma.

### 2.2 The Equivalent Source Method (ESM)

When performing the ESM calculation in the frequency domain the complex sound pressure values at $M$ microphones are expressed as

$$\mathbf{p}_m = \mathbf{A}\mathbf{q}\,, \tag{1}$$

where **q** is a vector of complex source strengths of the equivalent sources. The matrix, **A**, consist of monopole functions, i.e., Green's free space functions, and its (*m*,*n*) element is given as

$$[\mathbf{A}]_{mn} = \frac{e^{-jk|\mathbf{r}_m - \mathbf{r}_n|}}{|\mathbf{r}_m - \mathbf{r}_n|}. \tag{2}$$

Here, $\mathbf{r_m}$ and $\mathbf{r_n}$ are the locations of the microphones and equivalent sources, respectively, $k=\omega/c$ is the wavenumber and $c$ is the speed of sound. Equation (1) is typically underdetermined, meaning that there are more equivalent sources than microphones, but a unique solution can be found by solving it in a least squares sense as

$$\mathbf{q} = \left(\mathbf{A}^H\mathbf{A} + \lambda^2\mathbf{I}\right)^{-1}\mathbf{A}^H\mathbf{p_m}. \tag{3}$$

Tikhonov regularization has been introduced by the regularization parameter, λ, to prevent amplifications of noise components when solving the inverse problem. There are different techniques for estimating the optimal value of λ such as Generalized Cross Validation (GCV), L-curve or Morozov's Discrepancy Principle (9). In this paper, the latter technique will be applied.
Next, the computed source strengths can be used to estimate sound pressure and particle velocity on the actual surface as

$$\mathbf{p_s} = \mathbf{A_s}\mathbf{q} \tag{4}$$

and

$$\mathbf{v_s} = \mathbf{B_s}\mathbf{q} \tag{5}$$

where the elements of the matrix, $\mathbf{A_s}$, is similar to that of Equation (2) except now representing relations from equivalent source positions to points on the reconstruction surface. The elements of $\mathbf{B_s}$ are found by applying Euler's equation on the elements of $\mathbf{A_s}$.

## 3. MEASUREMENTS

### 3.1 Measurement Setup

A set of measurements has been carried out together with Denso Corporation on two different electrical motors. One of the motors is an outer rotor motor and results from those measurements are presented in Reference 10. This paper considers another results from another motor which is a brushless DC (BLDC) motor. The diameter of the housing is 8 cm and the full height is approximately 10 cm. Holography measurements were made by surrounding the motor by a cylindrical array that consists of four rings of microphones with 15 in each ring as shown in Figure 3a. The array has a diameter of 10 cm, the height was 6 cm and the top of the array was aligned with the top of the motor. For validation purpose measurements were also made with a laser Doppler vibrometer with the motor in the same condition. These measurements carried out with two lasers – one as a fixed reference and the other was manually moved point-by-point to cover the motor. A total of 45 laser positions were included corresponding to the positions of the lower three rings of microphones. Two additional signals were recorded during both array and laser measurements: an acceloremeter on the motor and an additional microphone a few centimeters from the motor. These were only included for cross checking purposes. The motor was running at 1650 RPM, because the measured sound pressure level was observed to increase around this RPM level. Denso provided a CAD geometry of the motor as seen in Figure 3b, and the model was meshed and given as input to the ESM algorithm.

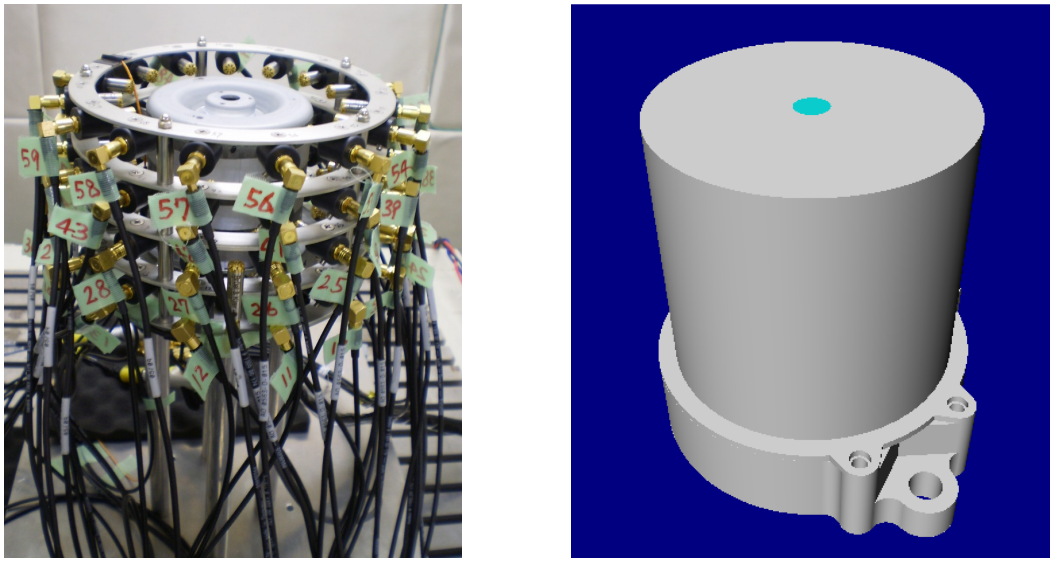

(a) (b)

Figure 3 – (a) Array measurement on a BLDC motor, and (b) CAD geometry of the motor.

### 3.2 Measurement Results

Before considering transient calculations, we make a stationary holography calculation based on cross spectra between the array microphones. Figure 4 shows the resulting particle velocity spectrum at a single point together with the autospectrum from the laser at the same point. In general, the two curves follow the same trend with the dominating peaks at the same frequencies. There are high levels at around 386 Hz, 800 Hz and 1925 Hzs. The 1925 Hz frequency corresponds well to the excitation of the resonance frequency of the stator, which is known to be at around 1926 Hz (see Reference 10). There are a few frequencies where only one of the methods detects high response. For instance at 150 Hz the laser has a high level that is not detected by holography. As mentioned, an extra reference microphone was included during both measurements, and Figure 5 shows the spectra of the corresponding sound pressure levels. Here, a peak is also observed near 150 Hz only during laser measurements, which shows that the sound field was not reproduced perfectly for the two measurement runs. When looking at the overall deflection shape from the laser measurement it was noticed that the motor had a rigid body movement at this frequency (not shown here), indicating that the vibration is related to the fixture of the motor rather than the modal properties of the motor. In other word, the modification to the setup such as mounting of the array could have influenced the mechanical properties of the setup thereby reducing the rigid body movement.

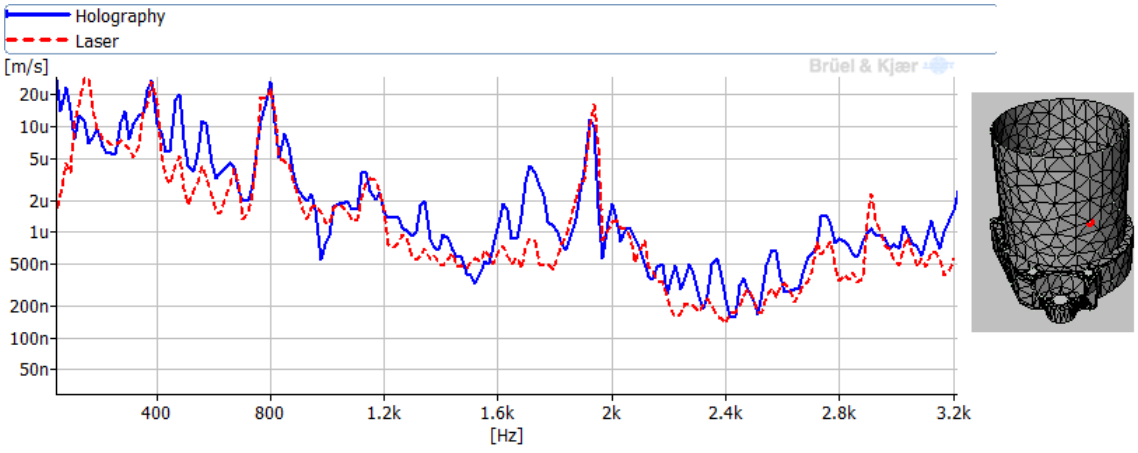


Figure 4 – Comparison of the velocity on the motor measured with holography and the laser, respectively. The frequency resolution is 16 Hz. The figure on the right hand side shows the location of the point.

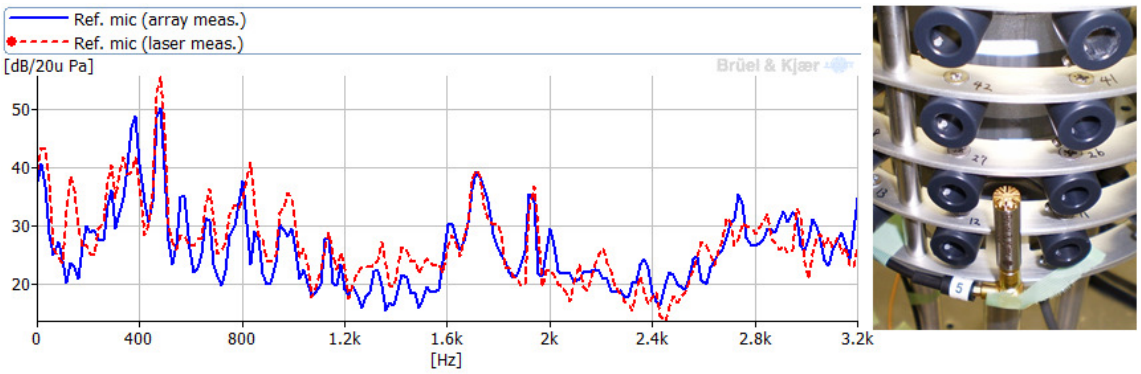


Figure 5 – Comparison of sound pressure level measured with the reference microphone close to the motor during array and laser measurements, respectively. The right hand side shows the location of the microphone.

Next, the non-stationary dataflow from Figure 2 is applied to the array data and the velocity is reconstructed in the time domain sample-by-sample for various frequency bands. It should be emphasized that the laser results are not using a time domain approach as such. Its complex output are simply found as the autospectrum of the laser signal (amplitude) and the phase of the cross spectras between the reference laser and the scanning laser (phase). The time dependency is then obtained by multiplying the complex output by $e^{j\omega t}$, and it is animated as a function of $t$. The holography data, on the other hand, represents the actual time domain, which means that it can also be used to analyze transient phenomena, whereas the laser approach assumes stationary conditions.

Figure 6 shows two snapshots at 110 Hz for holography and laser measurements, respectively. The results to the left corresponds to maximum deformation with its time defined as $t$=0 and the right hands side is at a time $t=T/2$ where $T$ is the time period of 110 Hz. The results in Figure 6 show very similar vibrational patterns with a rigid body movement. So again, the response is probably more due to the fixture than two the motor itself. As mentioned, the laser points did not include the upper ring of points on the motor, and that could explain why the the movement from the laser results looks more rigid that the holgraphy results, i.e., the high levels at the top were simply not included in the laser scan.

Figure 7 shows the velocity pattern at 800 Hz. Also at this frequency we see what seems to be a rigid body movement. The holography data shows that the lower part and the upper part of the motor is moving in opposite directions and there is a horizontal as well as a vertical nodal line.

Holography

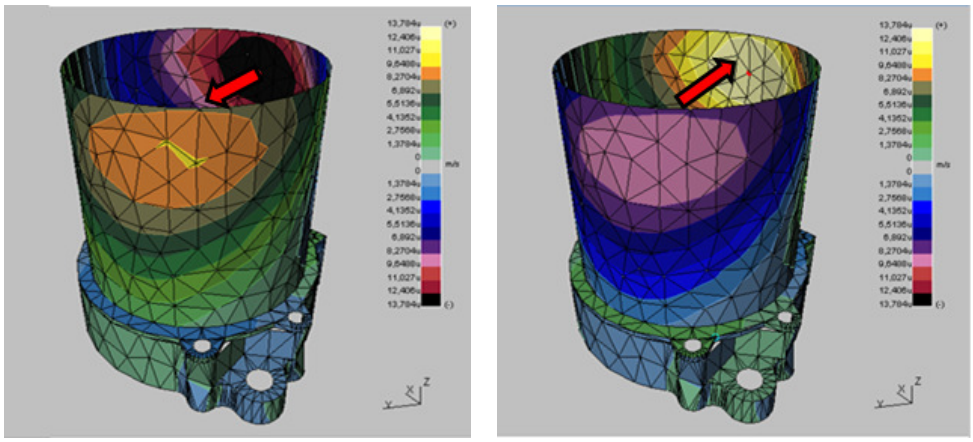

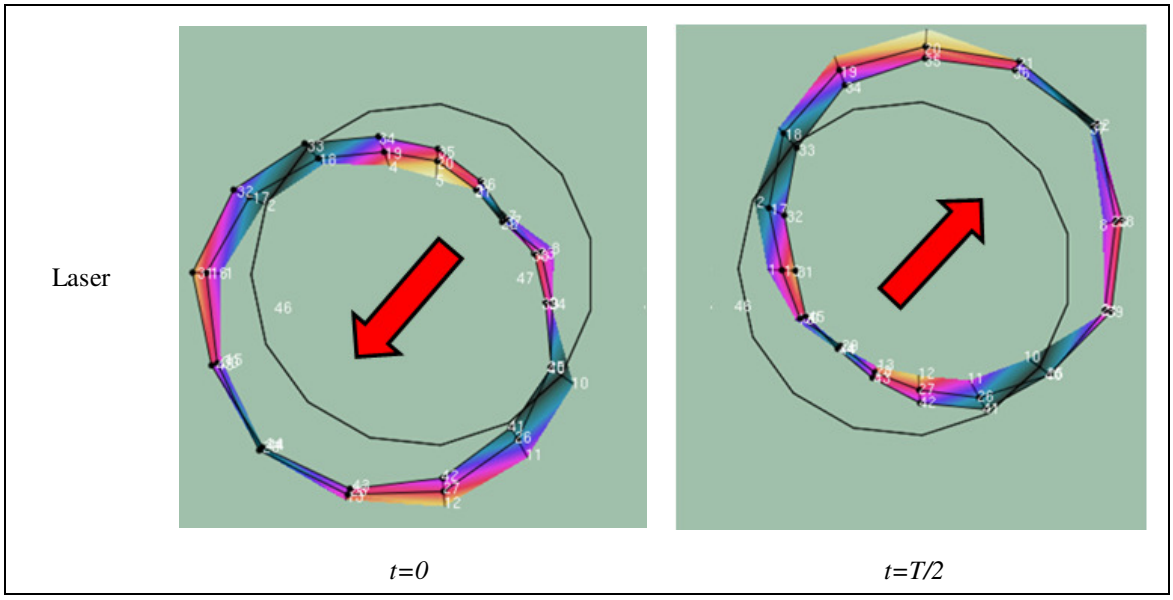


Figure 6 – Velocity reconstruction at 110 Hz at the two extreme deflections. Upper: 3D view of holography result. Lower: Laser result seen from above. The arrows indicate the direction of movement.

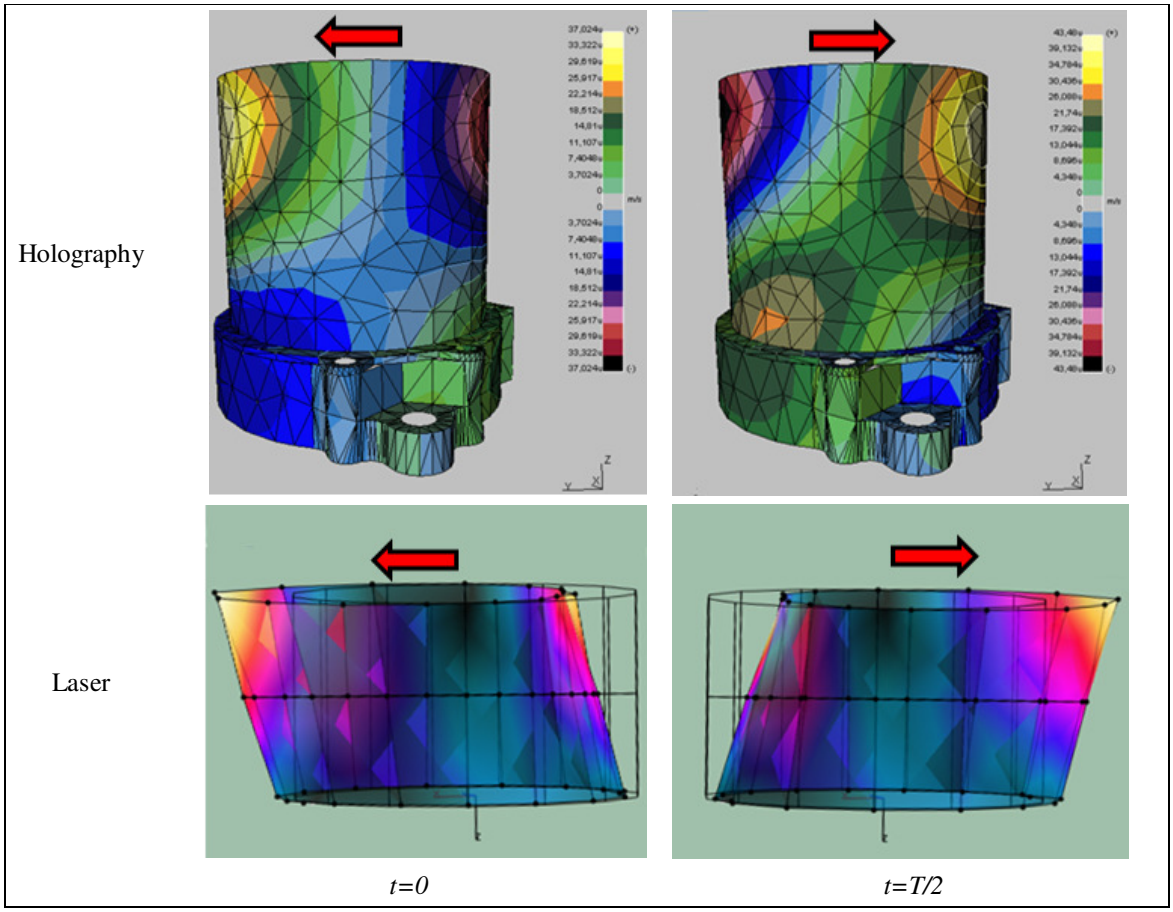


Figure 7 – Velocity reconstruction at 800 Hz at the two extreme deflections. Upper: 3D view of holography result. Lower: Laser result seen from the side. The arrows indicate the direction of movement.

It is sometimes difficult to get a full overview of the structural pattern when looking at 3D views. Figure 8 shows yet another comparison but this time the holography data is visualized on an unfolded mesh in 2D. The frequency is 1925 Hz which is one of the structural resonance frequencies of the motor. It is clearly seen that we are dealing with an elastic movement, i.e., the response is due to the actual motor and not the setup. Again, the two methods agree well on the shape of the deflection.

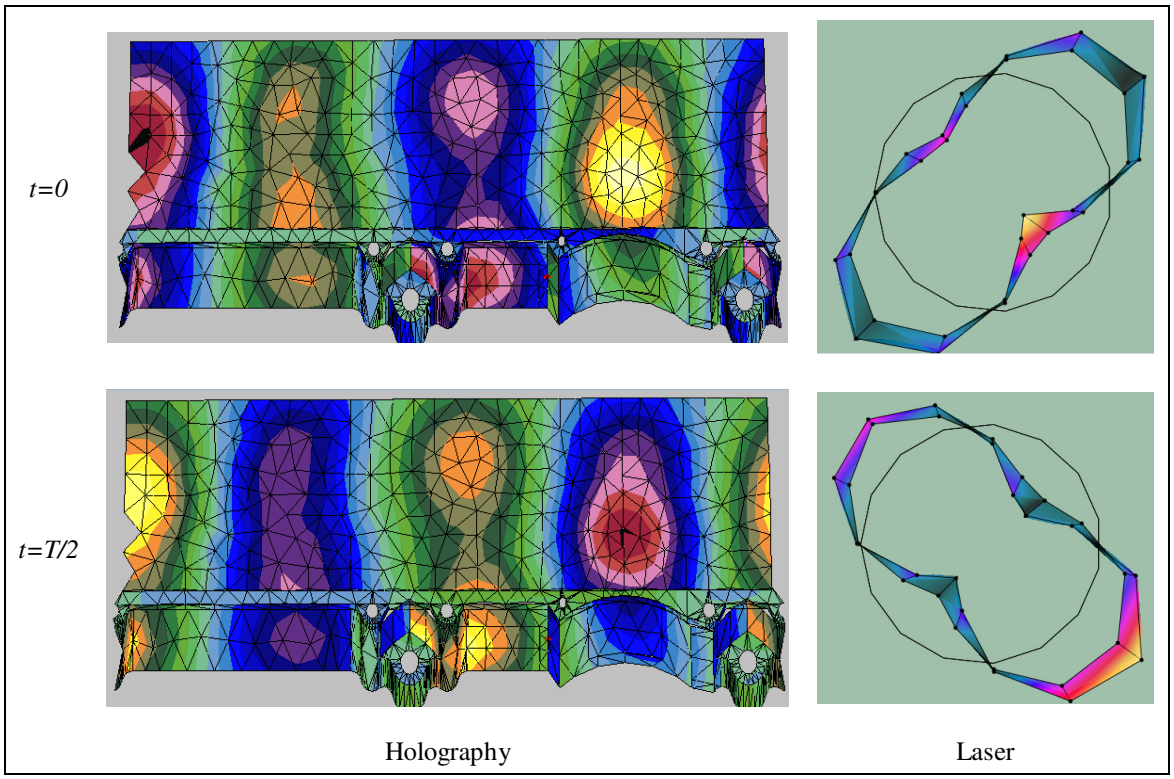


Figure 7 – Velocity reconstruction at 1925 Hz, Left: Holography with an unfolded mesh. Right: Laser results seen from above.

The final result to be presented here is shown in Figure 8. It is a stationary holography result covering the lower frequencies 168 Hz - 392 Hz Here we see that holography predicts a high level of vibration concentrated at one specific area. This behavior was not observed by the laser scan results. The location of the hotspot is where a metallic cable housing is mounted on the motor (see the right hand side of Figure 8). It is likely that the hotspot represents sound radiated from this cable housing, and since it is not included in the CAD model the high velocity is seen on the main part of the motor. It was also confirmed by looking at the raw pressure from the array microphones that there was a high sound pressure level around this area (not shown). The vibration of the housing probably does not excite the motor very much, which is why a similar pattern has not been seen for the laser results, and there were no laser scanning points directly on the housing.

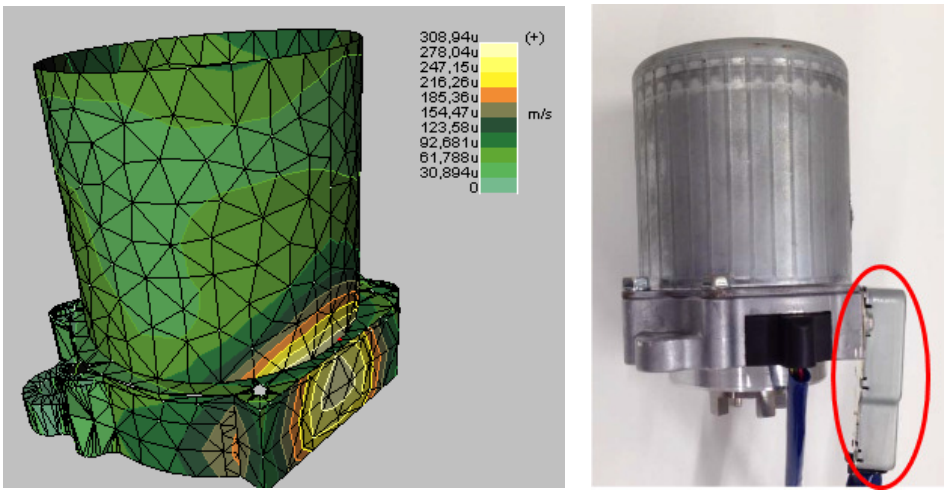


Figure 8 – Left: Velocity reconstructed holography. Frequency range: 168 Hz - 392Hz. Right: Picture of the motor with cable housing highlighted.

## 4. CONCLUSIONS

This paper describes a processing scheme for computing time histories of acoustical quantities such as particle velocity, sound pressure or displacement on an object of arbitrary shape. The processing applies a holography technique based on the Equivalent Source Method (ESM), which uses the pressure from an array of microphones that are located near the surface of interest and following the general geometrical trend of the source shape. The approach was demonstrated on a small electrical motor and the output was compared with a laser scan. The results showed very good agreement between laser and holography, and it was seen that the holography approach is indeed capable of reconstructing vibrations in time domain. In contrast to the laser scan measurements, holography does not assume stationary conditions, making it a very powerful technique for analysis of transient phenomena.

## ACKNOWLEDGEMENTS

The measurement facility and motor under test was kindly provided by Denso Corporation. The authors would like to thank Denso for the collaboration and especially Mr. Kazumasa Ikeda and Mr. Junichi Semura for valuable discussions and feedback.

## REFERENCES

1. Williams EG, Maynard JD, “Holographic Imaging without the wavelength resolution limit”, Phys. Rev. Lett., 45, 554-557, (1980).
2. Mingsian RB, “Application of BEM (boundary element method)-based acoustic holography to radiation analysis of sound sources with arbitrarily shaped geometries”, J. Acoust. Soc. Am., 92, 533-549, (1992).
3. Shuhmacher A, Hald J, Rasmussen KB, Hansen PC, "Sound source reconstruction using inverse boundary element calculations" J. Acoust. Soc. Am., 113, 114-127 (2003).
4. Sarkissian A, “Method of superposition applied to patch near-field acoustic holography,” J. Acoust. Soc. Am. 118, 671–678, (2005).
5. Valdivia N, Williams EG, “Study of the comparison of the methods of equivalent sources and boundary element methods for near-field acoustic holography,” J. Acoust. Soc. Am. 120, 3694–3705 (2006).
6. Saemann EU, Hald J, “Transient Tyre Noise Measurements Using Time Domain Holography,” 1997, Proc. SAE.
7. Hald J, “Time domain acoustical holography,” *Proceedings of Inter-noise 1995*.
8. Thomas JH, Grulier V, Paillasseur S, Pascal JC, Le Roux JC, “Real-time near-field acoustic holography for continuously visualizing nonstationary acoustic fields”, J. Acoust. Soc. Am. 128(6), 3554-3567 (2010).
9. Hansen PC, Rank-Deficient and Discrete Ill-Posed Problems: Numerical Aspects of Linear Inversion

(Society for Industrial and Applied Mathematics, Philadelphia, 1997).
10. Ikeda K, Semura J, Ohzawa T, "Mechnism of Noise Generation on Outer Rotor Motor," Proceedings of Internoise 2014.